

# *Supramolecular complexation between chain-folding poly(ester-imide)s and polycyclic aromatics: a fractal-based pattern of NMR ring-current shielding*

Article

Accepted Version

Knappert, M., Jin, T., Midgley, S. D., Wu, G., Scherman, O. A., Grau-Crespo, R. and Colquhoun, H. M. (2019) Supramolecular complexation between chain-folding poly(ester-imide)s and polycyclic aromatics: a fractal-based pattern of NMR ring-current shielding. *Polymer Chemistry*, 48. pp. 6641-6650. ISSN 1759-9954 doi: <https://doi.org/10.1039/c9py01460h> Available at <http://centaur.reading.ac.uk/87592/>

It is advisable to refer to the publisher's version if you intend to cite from the work. See [Guidance on citing](#).

To link to this article DOI: <http://dx.doi.org/10.1039/c9py01460h>

Publisher: Royal Society of Chemistry

All outputs in CentAUR are protected by Intellectual Property Rights law, including copyright law. Copyright and IPR is retained by the creators or other copyright holders. Terms and conditions for use of this material are defined in the [End User Agreement](#).

[www.reading.ac.uk/centaur](http://www.reading.ac.uk/centaur)

## **CentAUR**

Central Archive at the University of Reading

Reading's research outputs online

# Supramolecular complexation between chain-folding poly(ester-imide)s and polycyclic aromatics: a fractal-based pattern of ring-current shielding<sup>†</sup>

Marcus Knappert,<sup>a</sup> Tianqi Jin,<sup>a</sup> Scott D. Midgley,<sup>a</sup> Guanglu Wu,<sup>b</sup> Oren A. Scherman,<sup>b</sup> Ricardo Grau-Crespo<sup>a</sup> and Howard M. Colquhoun<sup>a\*</sup>

<sup>a</sup> *Department of Chemistry, University of Reading, Whiteknights, Reading, RG6 6AD, UK*

<sup>b</sup> *Melville Laboratory for Polymer Synthesis, Department of Chemistry, University of Cambridge, Lensfield Road, Cambridge CB2 1EW, UK*

**ABSTRACT:** Polycondensation of the diimide-based diols *N,N'*-bis(2-hydroxyethyl)hexafluoroisopropylidene-diphthalimide, *N,N'*-bis(2-hydroxyethyl)pyromellitimide, or *N,N'*-bis(2-hydroxyethyl)naphthalene-1,4,5,8-tetracarboxylic-diimide with aliphatic diacyl chlorides ClOC(CH<sub>2</sub>)<sub>x</sub>COCl ( $x = 1$  to 6) affords linear poly(ester-imide)s. Homopolymers based on hexafluoroisopropylidene-diphthalimide (HFDI) do not interact with polycyclic aromatics such as pyrene and perylene, as demonstrated by <sup>1</sup>H NMR spectroscopy. However, those containing pyromellitimide (PMDI) or 1,4,5,8-naphthalene-diimide (NDI) units residues show significant upfield complexation shifts of the diimide resonance in the presence of pyrene and perylene, consistent with supramolecular binding of the polycyclic aromatic molecules at the diimide residues. Poly(ester-imides) based on naphthalenediimide (NDI) units show particularly strong binding, with a pronounced maximum in complexation shift for the poly(ester-imide) with  $x = 2$ . Computational simulations (SCC-DFTB) suggest that this maximum is due to the presence of a chain fold at  $x = 2$  that is geometrically optimum for a pyrene molecule to bind between *pairs* of adjacent NDI residues, making near-van-der-Waals contact with both diimide units. Binding of this type was confirmed by <sup>1</sup>H NMR studies of pyrene complexation with a copoly(ester-imide) containing both NDI and HFDI units. The resulting NMR resonance-pattern shows clear evidence of fractal-type character.

---

<sup>†</sup> Electronic supplementary information (ESI) available:

## 1. Introduction

The ability of linear copolymers such as DNA and RNA to store and process digital sequence-information underpins the whole of biology.<sup>1,2</sup> However, no comparable information technology has yet been developed for molecular systems based on synthetic copolymers, even though the simplest AB copolymer is the logical equivalent of a binary string.<sup>3,4</sup> Nevertheless, significant progress towards such technology has been made in recent years,<sup>5</sup> especially with the development of sequence-specific polymerisation (i.e. sequence-writing) techniques.<sup>6-8</sup> In terms of "reading" copolymer sequences, it has been shown that tweezer-type reporter molecules with pyrene-based,  $\pi$ -electron-rich arms will bind to copolymers containing  $\pi$ -electron-poor pyromellitimide (PDI) or naphthalene-1,4,5,8-tetracarboximide (NDI) residues, via complementary  $\pi$ - $\pi$ -stacking.<sup>9,10</sup> This type of binding results in upfield shifts and splittings of  $^1\text{H}$  NMR resonances associated with the diimide residues, as a result of ring-current shielding by the complexed tweezer-molecules.<sup>10,11</sup> It has, moreover, been shown that *additive*, long range ring-current shielding by tweezer molecules bound further out along the chain increases the complexation shifts of NDI resonances, resulting in these shifts being highly sequence-dependent.<sup>11-13</sup> In addition, different tweezer-molecules were found to bind to different triplets, thereby producing a "frameshift" effect in the binding of longer sequences by multiple tweezer-molecules.<sup>14</sup>

More recently, it has been found that even simple non-tweezer molecules such as pyrene and perylene can produce sequence-dependent  $^1\text{H}$  complexation shifts in certain copolyimides where tight chain-folding enables the small molecule to bind *via* intercalation between two adjacent NDI residues.<sup>15</sup> Curiously, the resulting pattern of  $^1\text{H}$  NMR resonances showed a marked degree of *self-similarity*, and it was found that this reflected an underlying fractal distribution of ring-current shieldings produced by pyrene molecules binding to all the allowed sequences within which an NDI residue may be embedded.<sup>15</sup>

In a new investigation we have studied the binding of  $\pi$ -electron-rich aromatic molecules, specifically pyrene and perylene, to a novel series of homo- and co-poly(ester-imide)s containing strongly-binding NDI residues, weakly-binding PDI residues and/or non-binding hexafluoro-isopropylidene-diphthalimide (HFDI) sub-units. The work was undertaken because poly(ester-imide)s<sup>16-20</sup> have much greater future potential for "writing" sequence information (via catalytic ester-interchange) than the simpler, more chemically inert poly(ether-imide)s investigated previously.<sup>15</sup> In the present paper we report the discovery of an optimum poly(ester-imide) structure for chain-folding and pyrene-binding, identified by varying the diester spacer-unit between adjacent diimide (NDI) residues.

## 2. Experimental Section

### 2.1 Materials and Instrumentation

Starting materials, solvents, diacid chlorides ClCO(CH<sub>2</sub>)<sub>x</sub>COCl ( $x = 1-4$  and  $6-8$ ), and heptanedioic acid were purchased from Sigma-Aldrich, ThermoFisher or Fluorochem and were used as received. The diimide-based diols *N,N'*-Bis(2-hydroxyethyl)hexafluoro-isopropylidene-diphthalimide (**1**)<sup>21</sup> *N,N'*-bis(2-hydroxyethyl)-pyromellitimide (**2**),<sup>22</sup> and *N,N'*-bis(2-hydroxyethyl) naphthalene-1,4,5,8-tetracarboxylic diimide (**3**)<sup>23</sup> were synthesised as noted below. Proton and <sup>13</sup>C NMR spectra were recorded on a Bruker Nanobay 400 spectrometer (400 MHz for <sup>1</sup>H and 100 MHz for <sup>13</sup>C NMR) and on Bruker AVANCE 500 spectrometer with TCI Cryoprobe system (500 MHz for <sup>1</sup>H NMR). Proton chemical shifts ( $\delta$ ) are reported in ppm relative to tetramethylsilane (TMS,  $\delta = 0.00$  ppm), referred to residual <sup>1</sup>H solvent peaks, and <sup>13</sup>C NMR chemical shifts are similarly reported relative to TMS. Fourier transform infrared (FTIR) spectra were recorded on a Perkin Elmer 100 Spectrum FT-IR using a diamond ATR sampling accessory. Mass spectrometry was carried out using a ThermoFisher Scientific Orbitrap XL LCMS. Gel permeation chromatography (GPC) was

conducted using an Agilent Technologies 1260 Infinity system calibrated with polystyrene standards. Samples were dissolved in analytical grade THF (2 mg mL<sup>-1</sup>) containing BHT as stabiliser and run using the same solvent as the mobile phase, eluting through two Agilent PLgel 5 µm MIXED-D 300 × 7.5 mm columns in series. Phase transitions were identified by DSC under nitrogen, using a TA Instruments DSC 2920 or a Mettler Toledo DSC23e instrument. Melting points are quoted as peak temperatures and glass transitions as onsets. Weighed samples of ca. 5 mg of monomer or 10 mg of polymer were heated twice from 30 °C to 325 °C at a scan rate of 10 °C min<sup>-1</sup>. Inherent viscosities ( $\eta_{inh}$ ) were measured at 25 °C with 0.1% w/v solutions of polymer in chloroform/hexafluoropropan-2-ol (1:1, v/v) or in chloroform/trifluoroethanol (6:1, v/v) using a Schott Instruments CT 52 auto-viscometer with glass capillary No. 53103.

## 2.2 Computational methods

Pyrene binding (intercalation) energies were obtained using the self-consistent-charge density functional tight-binding (SCC-DFTB) approach, as implemented within the DFTB+ code.<sup>24</sup> Parameters for all atoms and pairs including elements C, H, N, O were taken from the “mio” parameter set of the Slater-Koster library.<sup>25</sup> Dispersion corrections based on a Lennard-Jones potential were applied in all simulations.<sup>26</sup> Each polymer was modelled as a discrete heptameric oligomer, and the intercalation energy of pyrene was evaluated at the central chain-fold. Intercalation energies ( $E_{int}$ ) were derived using the expression:

$$E_{int} = E_{complex} - (E_{pyrene} + E_{polymer})$$

where  $E_{complex}$ ,  $E_{pyrene}$  and  $E_{polymer}$  are the minimised energies of the polymer/pyrene complex, the free pyrene molecule, and the non-intercalated polymer, respectively.

Simulations of <sup>1</sup>H NMR spectra were carried out using the "peak tabel to spectrum" script within *Mnova* (version 14, Mestrelab Research, Santiago).

### 2.3 Monomer synthesis

*N,N'*-Bis(2-hydroxyethyl)hexafluoroisopropylidene-diphthalimide (**1**):

4,4'-Hexafluoroisopropylidenediphthalic dianhydride (25.32 g, 57.0 mmol) was dissolved in a mixture of *N,N*-dimethylacetamide (50 mL), 2-aminoethanol (7.38 g, 120.8 mmol) and toluene (30 mL). The solution was heated at reflux for 17 h with Dean-Stark removal of water. After being cooled to room temperature, the solution was precipitated into water (350 mL) and the solid filtered off and dried for 24 h at 100 °C, affording a crude product (27.51 g, 91%). This was recrystallised from *n*-butanol (53 mL) and the solution was stored at 5 °C for two weeks until crystallisation was complete. The product was filtered off, washed with water and ethanol (three times each) and dried at 100 °C for 24 h to afford pure diol **2** (25.69 g, 85% yield). M.p. 212 °C. <sup>1</sup>H NMR (400 MHz, DMSO-*d*<sub>6</sub>) δ<sub>H</sub> 8.07 (d, J = 8.0 Hz, 2H<sub>i</sub>), 7.89 (d, J = 8.1 Hz, 2H<sub>h</sub>), 7.65 (s, 2H<sub>f</sub>), 4.83 (t, J = 6.1 Hz, 2H<sub>a</sub>), 3.66 (t, J = 5.5 Hz, 4H<sub>c</sub>), 3.59 (m, 4H<sub>b</sub>). ESI MS *m/z* = 553.0782 [M+Na]<sup>+</sup>; calculated 553.0805.

*N,N'*-Bis(2-hydroxyethyl)pyromellitimide (**2**):

2-Aminoethanol (4.0114 g, 65.7 mmol) was added to a mixture of *N,N*-dimethylacetamide (15 mL), toluene (35 mL) and pyromellitic dianhydride (7.1066 g, 32.6 mmol). The solution was heated at reflux for 16 h, and the water formed in the reaction was removed by azeotropic distillation using a Dean-Stark apparatus. The system was then cooled to room temperature and the product was precipitated in deionised water, filtered off, and washed three times with water and methanol and dried in an oven at 100 °C for 24 h to afford a crude product (6.730 g, 68%). This was recrystallised from a mixture of DMF (22.5 mL) and water (22.5 mL) and, after cooling at 5 °C overnight, the product was filtered off and washed three times each with water and ethanol. It was finally dried in an oven at 100 °C for 24 h to afford pure, crystalline diol **1** (4.953 g, 50% overall yield). M.p. 282 °C. <sup>1</sup>H NMR (400 MHz,

DMSO-*d*<sub>6</sub>)  $\delta_{\text{H}}$  8.21 (s, 2H, H<sub>f</sub>), 4.89 (t, *J* = 6.1 Hz, 2H<sub>a</sub>), 3.71 (t, *J* = 5.7 Hz, 4H<sub>c</sub>), 3.63 (q, *J* = 5.7 Hz, 4H<sub>b</sub>). ESI MS *m/z* = 327.0587 [M+Na]<sup>+</sup>, calculated 327.0588.

*N,N'*-Bis(2-hydroxyethyl)naphthalene-1,4,5,8-tetracarboxylic diimide (**3**):

1,4,5,8-Naphthalenetetracarboxylic dianhydride (50.61 g, 188.7 mmol) was dissolved in a mixture of *N,N*-dimethylacetamide (250 mL), 2-aminoethanol (25.03 g, 409.8 mmol) and toluene (30 mL). The solution was heated to reflux for 16 h with Dean-Stark removal of water. After cooling to room temperature, the precipitated crystals were filtered off and washed with water, acetone and methanol (three times each). The crystals were dried at 100 °C for 24 h to afford a crude product which was recrystallised in ca. 6 g batches from a mixture of *N,N*-dimethylformamide (145 mL), *N,N*-dimethylacetamide (75 mL) and H<sub>2</sub>O (5 mL). After crystallisation at 5 °C overnight, the crystals were filtered off, washed with water and ethanol (three times each) and finally dried at 100 °C for 24 h to afford pure diol **3** (total yield 58.8 g, 86% yield). M.p. 290 °C. <sup>1</sup>H NMR (400 MHz, DMSO-*d*<sub>6</sub>)  $\delta_{\text{H}}$  8.59 (s, 4H, C-H, f), 4.86 (t, *J* = 6.1 Hz, 2H, a), 4.16 (t, *J* = 6.4 Hz, 4H<sub>c</sub>), 3.66 (q, *J* = 6.3 Hz, 4H<sub>b</sub>). ESI MS *m/z* = 377.0744 [M+Na]<sup>+</sup>, calculated 377.0749.

*Heptanedioyl dichloride*

Heptanedioic acid (65.5 g, 409 mmol) was dissolved in thionyl chloride (400 mL) and the mixture was refluxed for 4 h. The excess of thionyl chloride was evaporated under vacuum and the residual brown oil was purified by distillation at reduced pressure (2 mbar) affording heptanedioyl dichloride as a colourless liquid (57.2 g, 71% yield). <sup>1</sup>H NMR (400 MHz, CDCl<sub>3</sub>)  $\delta$  (ppm) = 2.91 (t, *J* = 7.2 Hz, 4H), 1.73 (m, 4H), 1.49–1.36 (m, 2H).

## 2.4 Polymer synthesis: representative procedure

1,2-Dichlorobenzene (4.5 mL, distilled from CaH<sub>2</sub>), *N,N'*-bis-(2-hydroxyethyl)-naphthalene tetracarboxylic diimide (dried at 120 °C for 24 h; 2.09 g, 5.90 mmol) and adipoyl chloride,



CICO(CH<sub>2</sub>)<sub>4</sub>COCl (1.09 g, 5.96 mmol), were stirred under nitrogen at room temperature and the mixture was heated to 170 °C for 24 h with a slow dinitrogen purge to remove the evolved hydrogen chloride. After cooling to room temperature the reaction mixture was dissolved in dichloromethane/hexafluoroisopropanol (1:1, v/v, 30 mL) and added dropwise into an excess of methanol (400 mL). The precipitate was filtered off, washed with methanol and dried at 80 °C for 24 h. The reprecipitation was repeated three times to afford pure polymer (2.10 g, 76%). Variations from this procedure for specific polymers are noted in Table 1, and full synthetic details are given in the ESI.

## 2.5 Polymer characterisation

Poly(ester-imide)s **4–25** were characterised by <sup>1</sup>H and <sup>13</sup>C NMR spectroscopy, IR spectroscopy, DSC and solution viscometry. Results are summarised in Table 1 and detailed in the ESI. Gel permeation chromatography in THF was possible for homopolymers **4** and **5**, derived from 4,4'-hexafluoroisopropylidenediphthalic dianhydride, but all the other polymers described here were insoluble in conventional GPC solvents and so were characterised by solution viscometry in the proton-donor solvent system chloroform/trifluoroethanol (6:1, v:v). However, the GPC data for **4** and **5** enabled construction of a calibration plot of inherent viscosity against *M<sub>n</sub>* (see ESI) and, from this plot, an estimate of *M<sub>n</sub>* for the poly(ester-imide)s reported here could be obtained.

## 3. Results and discussion

### 3.1 Synthesis of poly(ester-imide)s

The aim of the present work was to evaluate the possibility of supramolecular complexation of small molecules with poly(ester-imide)s via chain-folding and complementary  $\pi$ - $\pi$ -stacking. We have previously shown that supramolecular processes of this type lead to



### 3.2 Interactions of poly(ester-imide)s with polycyclic aromatics

It is well established that complexation of certain polyimides by aromatic molecules such as pyrene and perylene, via complementary  $\pi$ - $\pi$ -stacking, leads to substantial upfield complexation shifts of  $^1\text{H}$  NMR resonances associated with the diimide residues as a result of magnetic ring-current shielding by the complexed aromatic.<sup>9-15</sup> Although the forces involved in complementary  $\pi$ - $\pi$ -stacking remain a matter for discussion, it is clear that this type of supramolecular complexation is favoured by coplanarity of the diimide residues, as in PMDI and NDI, and strongly disfavoured by non-planar and/or sterically-hindered diimide units such as HFDI.

**Table 1.** Polymer synthesis and characterisation <sup>a</sup>

| Polymer Ref. No. | Diimide monomer   | $x$ in $(\text{CH}_2)_x$ <sup>d</sup> | Reaction Solvent     | Temp. °C | Time h | $\eta_{\text{inh}}$ dL g <sup>-1</sup> | $M_n$ daltons | $\mathcal{D}$ | $T_g$ °C | $T_m$ °C |
|------------------|-------------------|---------------------------------------|----------------------|----------|--------|--|---------------|---------------|----------|----------|
| <b>4</b>         | HFDI <sup>a</sup> | 3                                     | 1,2-DCB <sup>e</sup> | 120      | 4      | 0.83                                   | 30,200        | 2.07          | 109      | -        |
| <b>5</b>         | HFDI              | 5                                     | 1-CNp <sup>f</sup>   | 120      | 4      | 0.56                                   | 20,400        | 1.92          | 72       | -        |
| <b>6</b>         | PMDI <sup>b</sup> | 1                                     | 1,2-DCB              | 170      | 24     | 0.48                                   | -             | -             | -        | 194      |
| <b>7</b>         | PMDI              | 2                                     | 1,2-DCB              | 170      | 24     | 0.36                                   | -             | -             | -        | 233      |
| <b>8</b>         | PMDI              | 3                                     | 1,2-DCB              | 170      | 24     | 0.60                                   | -             | -             | -        | 223      |
| <b>9</b>         | PMDI              | 4                                     | 1,2-DCB              | 170      | 24     | 0.55                                   | -             | -             | -        | 253      |
| <b>10</b>        | PMDI              | 5                                     | 1,2-DCB              | 170      | 24     | 0.59                                   | -             | -             | -        | 190      |
| <b>11</b>        | PMDI              | 6                                     | 1,2-DCB              | 170      | 24     | 0.62                                   | -             | -             | -        | 217      |
| <b>12</b>        | PMDI              | 7                                     | 1,2-DCB              | 170      | 24     | 0.37                                   | -             | -             | -        | 203      |
| <b>13</b>        | PMDI              | 8                                     | 1,2-DCB              | 170      | 24     | 0.59                                   | -             | -             | -        | 207      |
| <b>14</b>        | NDI <sup>c</sup>  | 1                                     | 1,2-DCB              | 170      | 24     | 0.17                                   | -             | -             | 189      | -        |
| <b>15</b>        | NDI               | 2                                     | 1,2-DCB              | 170      | 24     | 0.56                                   | -             | -             | 139      | -        |
| <b>16</b>        | NDI               | 3                                     | 1,2-DCB              | 170      | 24     | 1.54                                   | -             | -             | 132      | -        |
| <b>17</b>        | NDI               | 4                                     | 1,2-DCB              | 170      | 24     | 0.75                                   | -             | -             | 116      | -        |
| <b>18</b>        | NDI               | 5                                     | 1,2-DCB              | 170      | 24     | 0.58                                   | -             | -             | 90       | -        |
| <b>19</b>        | NDI               | 6                                     | 1,2-DCB              | 170      | 24     | 0.19                                   | -             | -             | 73       | -        |
| <b>20</b>        | NDI               | 7                                     | 1,2-DCB              | 170      | 24     | 1.20                                   | -             | -             | 76       | -        |
| <b>21</b>        | NDI               | 8                                     | 1,2-DCB              | 170      | 24     | 0.93                                   | -             | -             | 50       | -        |
| <b>22</b>        | NDI/<br>HFDI      | 2                                     | 1-CNp                | 160      | 24     | 0.20                                   | -             | -             | 130      | -        |
| <b>23</b>        | NDI/<br>HFDI      | 3                                     | 1-CNp                | 160      | 24     | 0.26                                   | -             | -             | 99       | -        |

<sup>a</sup> Full details in ESI. *N,N'*-bis-(2-hydroxyethyl)hexafluoroisopropylidene dipthalimide. <sup>b</sup> *N,N'*-bis-(2-hydroxyethyl)pyromellitic diimide. <sup>c</sup> *N,N'*-bis-(2-hydroxyethyl)-1,4,5,8-naphthalenediimide. <sup>d</sup> in diacid chloride  $\text{ClOC}(\text{CH}_2)_x\text{COCl}$ . <sup>e</sup> 1,2-dichlorobenzene. <sup>f</sup> 1-chloronaphthalene.

Thus, the HFDI-based poly(ester-imide)s **4** and **5** (4 mM solutions based on diimide residues) showed no detectable  $^1\text{H}$  complexation shifts in the presence of pyrene or perylene (2 equivalents per diimide residue), whereas the PMDI-based polymers **6** to **13** showed small but consistent upfield shifts (ca. 0.1 ppm) of their PMDI resonances under the same conditions. There was, however, no significant dependence of the complexation shift on the length of the diester-linkage between adjacent PMDI residues (see ESI). In contrast, the NDI resonances in polymers **14** to **21** showed substantial complexation shifts in the presence of 2 equivalents of pyrene, the shifts varying markedly (from 0.20 to 0.75 ppm at 8 mM concentration of NDI residues) with the length of the diester-spacer  $[-\text{OOC}(\text{CH}_2)_x\text{COO}-]$ . Polymer-pyrene binding evidently occurs under fast-exchange conditions on the NMR time scale as separate resonances corresponding to bound and unbound NDI residues are not observed, even at sub-stoichiometric pyrene:NDI ratios. The complexation shift reached a maximum at  $x = 2$ , and the same trend was found for complexation of perylene which showed even more pronounced complexation shifts (Figure 2). Charge-transfer absorptions resulting from polyimide complexation produce strongly coloured solutions – deep red with pyrene and an intense dark green for perylene.

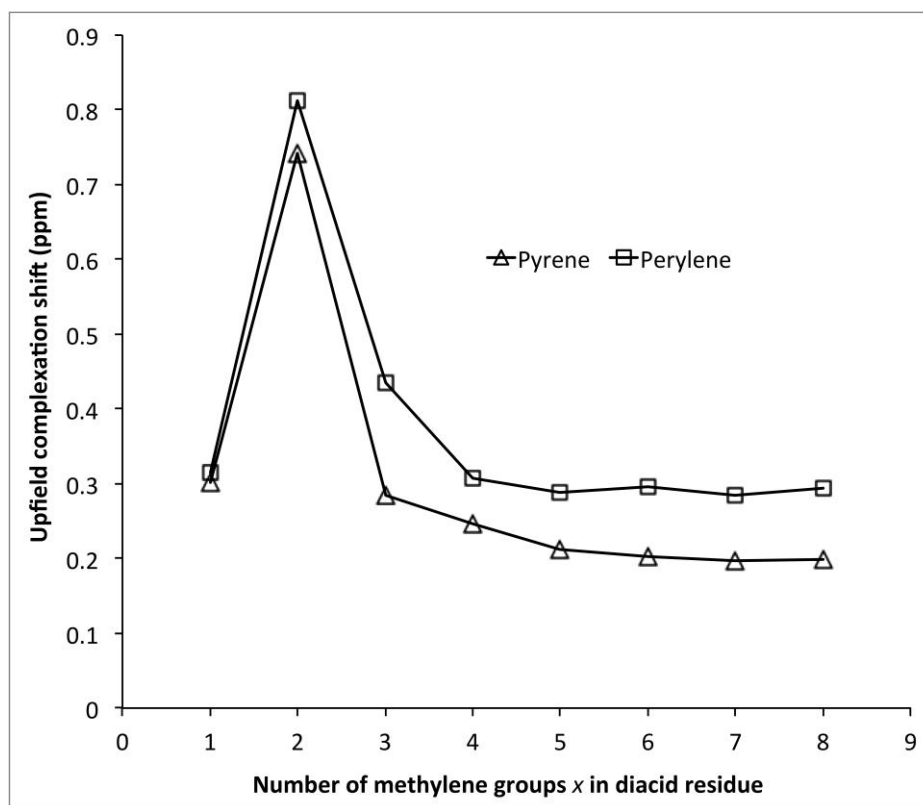


**Figure 2.** Complexation shifts for NDI-based poly(ester-imide)s **14** – **21** [8 mM in NDI, in  $\text{CDCl}_3/\text{TFE}$  (6:1 v/v)] in the presence of 2 mol. equiv. per NDI of pyrene- $d_{10}$  ( $\triangle$ ) or perylene- $d_{12}$  ( $\square$ ).

### 3.3 Computational simulation of pyrene-binding

In the light of previous work showing that strong complexation of pyrene by poly(ether-imide)s was associated with chain-folding and binding of the small molecule by intercalation between two neighbouring NDI residues,<sup>15</sup> it seemed possible that the maximum in pyrene binding at  $x = 2$  results from the polymer with this spacer adopting a chain-fold geometry that is especially favourable for binding. Computational simulation (SCC-DFTB with dispersion correction) of pyrene complexation by polymers **14** ( $x = 1$ ) **15** ( $x = 2$ ) and **18** ( $x = 5$ ) provided strong support for this idea, with computed binding energies for pyrene indeed being greatest at  $x = 2$ , as shown in Figure 3. The polymers were modelled as heptamers, with the energies of binding being calculated for a pyrene molecule intercalating at the central chain-fold.

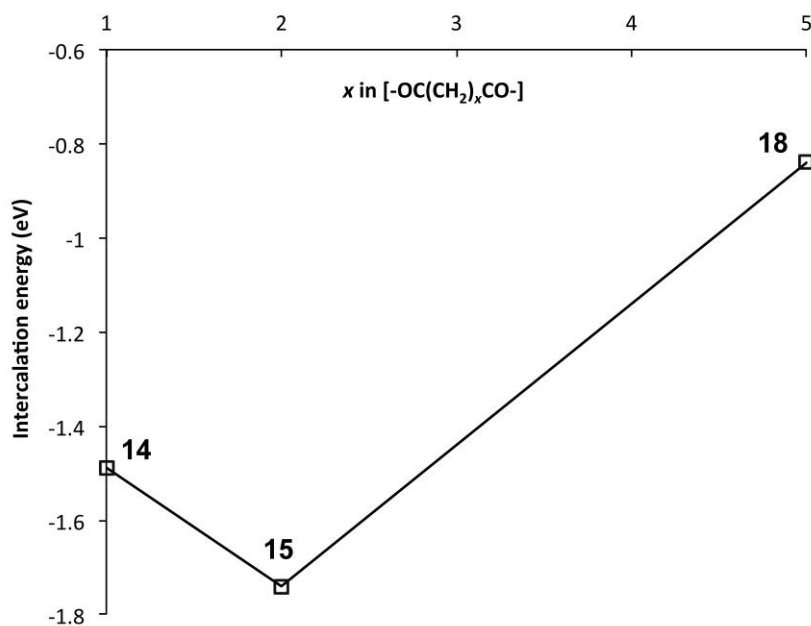


**Figure 3.** Computed intercalation energies for the binding of pyrene to poly(ester-imide)s **14** ( $x = 1$ ) **15** ( $x = 2$ ) and **18** ( $x = 5$ ). More negative energy-values correspond to stronger binding.

A rationale for these results can be seen immediately by inspection of Figure 4, which shows space-filling (van der Waals radii) models of energy-minimised chains for the three different values of  $x$ , in the presence of an intercalating pyrene molecule. For  $x = 1$  the chain is seen to fold regularly, with near-parallel NDI subunits, but the average C-C distance between equivalent NDI carbons at the "binding" chain fold of 8.14 Å (range 8.00 to 8.27 Å) is clearly too great for pyrene to make simultaneous van der Waals contact with both NDI residues. For  $x = 2$ , however, the chain-fold is tighter and the gap between neighbouring NDI residues is smaller (average 7.59 Å), even though the diester spacer is longer and the binding residues are tilted slightly towards one other (contact range 6.67 to 8.50 Å). The heptameric chain, overall, is noticeably contracted relative to the corresponding chain where  $x = 2$  (Figure 4) and the intercalating pyrene makes much closer contact with both adjacent NDI residues. Finally, when  $x = 5$ , the chain folding is distinctly irregular, and the NDI-NDI spacing at the "binding" chain fold is greatly expanded to give an average C-C spacing of 10.02 Å (range

9.80 to 10.24 Å). The trend in binding strength for polymers **14**, **15** and **18**, where  $x = 1$ , 2 and 5 respectively, is thus quite reasonably accounted for.

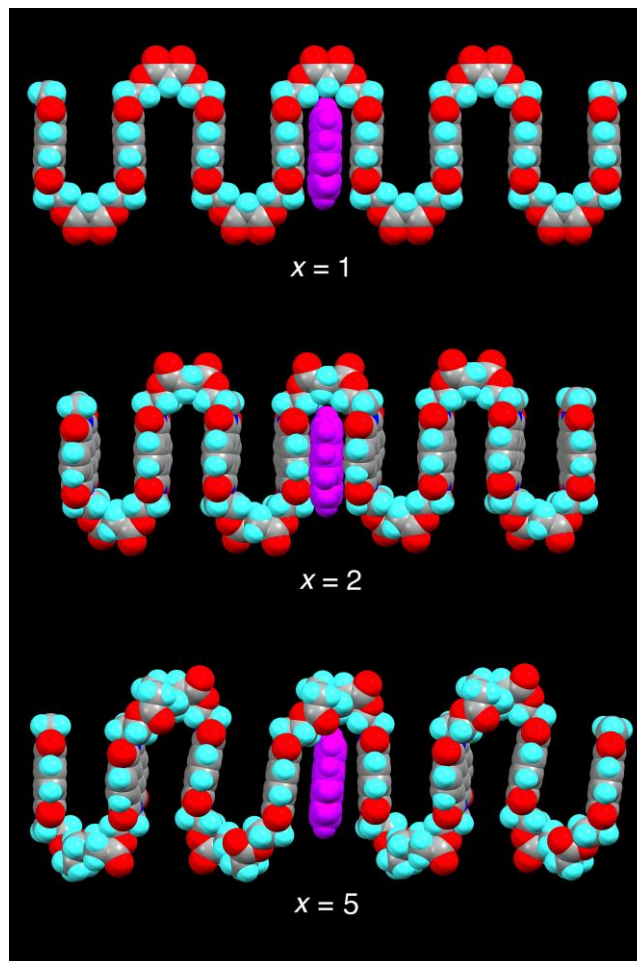


**Figure 4.** Energy-minimised geometries (SCC-DFTB with dispersion correction) for pyrene complexes of the NDI-based poly(ester-imide)s **14**, **15** and **18**, modelled as heptamers. The optimum fit for  $\pi$ - $\pi$ -stacking of pyrene at  $x = 2$  (polymer **15**) is very clear.

### 3.4 Sequence-specific binding in a co-poly(ester-imide)

Our earlier work on sequence-dependent polymer complexation with pyrene showed that an NDI copolyether containing equal proportions of strongly-binding and weakly-binding chain folds (Figure 5a/b) gave, in the presence of pyrene, a  $^1\text{H}$  NMR spectrum containing a characteristic set of NDI resonances that each corresponded to a specific NDI-centred

sequence or group of sequences.<sup>15</sup> This resonance pattern was shown to result from intercalation of pyrene at tight chain-folds formed by pairs of NDI residues linked by triethylene-dioxy spacer units (Figure 5a), and the pattern could in fact be accounted for on the basis that binding at any other NDI residue in the chain was negligible by comparison. Moreover, the NMR spectrum itself was found to have elements of *self-similarity*, arising from an underlying fractal distribution of ring-current shieldings produced by pyrene-intercalation at all possible NDI-centred sequences.<sup>15</sup> In the present poly(ester-imide)s, an analogous situation could exist for the 1:1 copolymer containing bis(oxyethyl)-NDI and -HFDI residues linked by the succinate spacer ( $x = 2$ , copolymer **22**), as shown in Figure 5.

On the basis that, in copolymer **22**, we can identify a pair of adjacent NDI residues as a strongly-binding site, and ignore binding at other positions on the chain, it is possible to assign a digital code to each NDI-centred sequence. This code describes the location and number of binding sites relative to the central NDI residue. For example, denoting NDI residues as "I" and HFDI residues as "F", the quintet sequence IFIII has **one** "II" pair adjacent to (and including) the central "I" and **one** pair at a next-adjacent position. It is therefore assigned the code 11. The sequence IFIFI, in contrast, has **zero** "II" pairs adjacent to the centre, and **zero** pairs at the next-adjacent position, so this sequence would be assigned the code 00. Table 2 shows all sixteen possible I-centred quintet sequences and their assigned two-digit codes. There are nine possible combinations of 0, 1 and 2, taken in twos, but three of these (01, 02 and 12) are unused because they do not represent any of the sixteen possible quintet sequences. The table also shows that four of the six assigned codes are degenerate, i.e. they represent more than one sequence: much of this degeneracy arises from the fact that mirror-image sequences (shown side-by-side in Table 2) are indistinguishable by NMR.



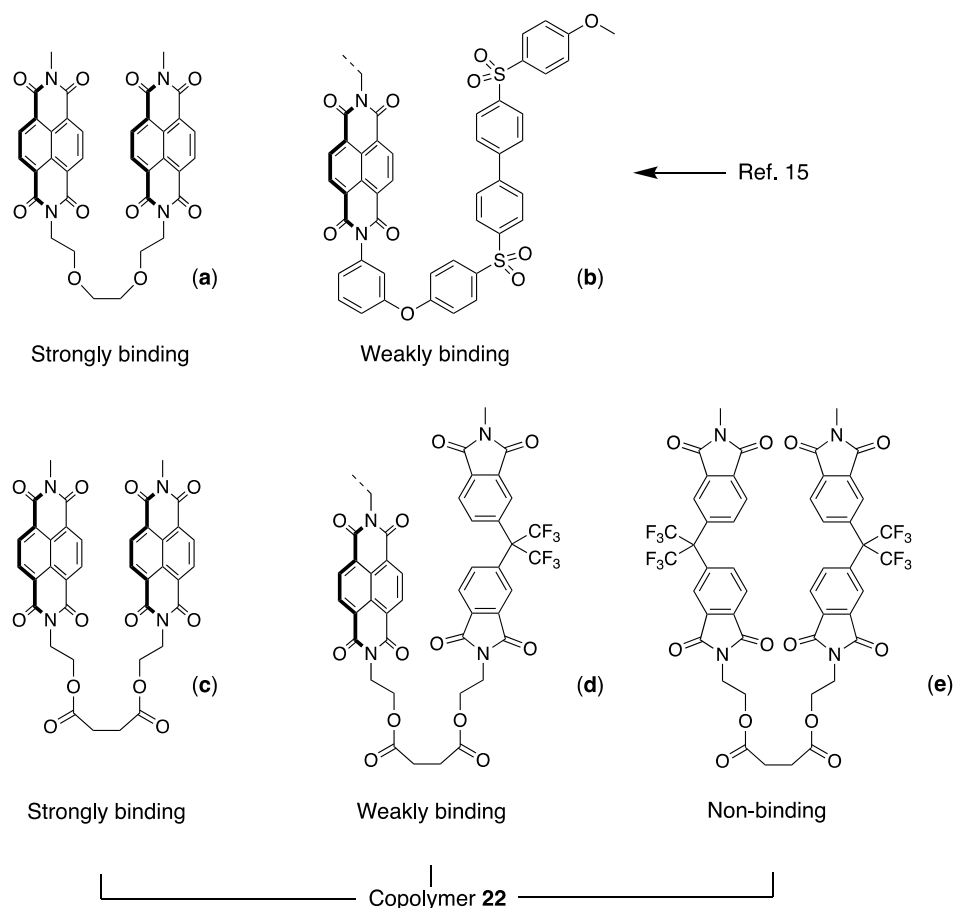


**Figure 5.** (a) Possible chain folds in: (a)/(b) the copoly(ether-imide) described in reference 15; and (c)/(d)/(e) copoly(ester-imide) **22** (this work).

The significance of these digital codes is that, as described in an earlier paper,<sup>15</sup> they can be used to predict the total ring-current shielding of a central NDI residue any given sequence in a chain-folding copolyimide. Such shielding, is additive, with an empirical "fall-off factor" of about four as an aromatic molecule (typically pyrene or perylene) binds at chain-folds further and further out from the central diimide residue. The system is digital rather than analogue because there are no intermediate binding positions between successive chain folds, and also because there are just three possibilities (0, 1 or 2) for the number of pyrene molecules bound at any specific distance (viewed in both directions) from the central "observed" NDI residue.

**Table 2.** The sixteen possible NDI-centred quintet sequences (shown in black) in the binary (I/F) copolymer **22**. As noted above, "I" = NDI and "F" = HFDI, and the assigned two-digit binding code (shown in blue) for each sequence reflects the location and number of adjacent II pairs. The six codes shown in blue are those that emerge from this assignment process; those shown in red do not emerge from any possible quintet sequence. Numbers in blue ( $T = \dots$ ) are total shielding factors for the originating sequences, calculated from Equation 1 with the value of  $a$  set to unity.

|          | <b>0</b>   | <b>1</b>  | <b>2</b>                                    |
|----------|--|---|---|
| <b>0</b> | <b>00 (<math>T = 0</math>)</b><br>FFIFF<br>FFIFI, IFFIF<br>IFIFI | 01  | 02  |
| <b>1</b> | <b>10 (<math>T = 0.25</math>)</b><br>FFIIF, FIIFF<br>FIFI, IFIIF | <b>11 (<math>T = 0.3125</math>)</b><br>FFIII, IIIFF<br>IFI, IIIFI | 12  |
| <b>2</b> | <b>20 (<math>T = 0.5</math>)</b><br>FIIIF                        | <b>21 (<math>T = 0.5625</math>)</b><br>FIIII, IIIIF               | <b>22 (<math>T = 0.625</math>)</b><br>IIIII |

Using the above concepts, it can be shown that the **total** (relative) ring current shielding,  $T$ , of a central NDI residue by pyrene molecules intercalating into a specific binary copolymer sequence can be described quantitatively by Equation 1:

$$T = a \sum_{k=1}^{k_{\max}} \frac{N_k}{4^k}$$

**Equation 1**

where  $k$  represents the location of *potential* binding sites relative to the centre ( $k = 1$  for the two sites immediately adjacent to (and including) the central NDI residue;  $k = 2$  for the next-adjacent two sites, and so on).<sup>15</sup> The coefficient  $N_k$  is the number of *actual* binding sites for each value of  $k$ :  $N_k$  is thus equal to the corresponding digit (0, 1 or 2) in the code for the sequence being considered. The highest value of  $k$  in the summation, identified as  $k_{\max}$ , is the number of different types of position in any sequence-length (relative to the central "I") where "II" pairs might be found. Thus, for quintet sequences  $k_{\max}$  is 2, for septets 3, for

nonets 4 and so on. The pre-summation factor  $a$  is a linear scaling term to allow the dimensionless shielding factor  $T$  to be converted empirically into a complexation shift in ppm. For a previous copolymer-pyrene complex the value of  $a$  was found to be very close to 1, but no physical significance could be attached to this as  $a$  is concentration-dependent (see below). As an example of Equation 1, the quintet sequence IIIIF gives rise to the code 21 (Table 2), and summing the individual contributions to shielding for this sequence we obtain  $T = 2/4^1 + 1/4^2 = 0.5625$ . Similarly, sequence FFIIF is represented by code 10, from which  $T = 1/4^1 + 0/4^2 = 0.25$ . Total shielding factors  $T$ , from Equation 1, are given in Table 2 for all the possible quintet sequences present in copolymers **22**. These can be used as predictors of relative complexation shifts (see below).

### 3.5 Fractal character of ring-current shieldings

We have shown previously<sup>15</sup> that Equation 1 (with  $a = 1$  and  $k_{\max} = \infty$ ) defines a mathematical fractal known as the fourth-quarter Cantor set, even though it was actually discovered by Smith.<sup>27</sup> The set represented by Equation 1 can (like many fractals) also be constructed geometrically. In the present case, a line of unit length is divided into four equal segments and the right hand (fourth) segment is discarded. These two operations are then repeated on the remaining three segments, and so on indefinitely. See Figure 6. In copolymer terms, successive iterations of this construction correspond to increasing the length of the copolymer sequence being considered.<sup>15</sup> Thus the first iteration yields three segments corresponding – in a copolymer containing only NDI ("I") and HFDI ("F") residues – to the three distinguishable triplet sequences FIF, [FII+IIF] and III. The latter sequences contain 0, 1 and 2 "II" pairs respectively and the corresponding segments are thus labelled 0, 1 and 2. The second iteration of the construction yields nine segments labelled 00, 01, 02 etc., corresponding to the nine possible combinations of 0, 1 and 2 taken in pairs, as shown in Table 2. However, Table 2 also demonstrates that only six of these nine combinations

correspond to actual and distinguishable F/I quintets, so just six quintet-based resonances are predicted by the model (Figure 6).

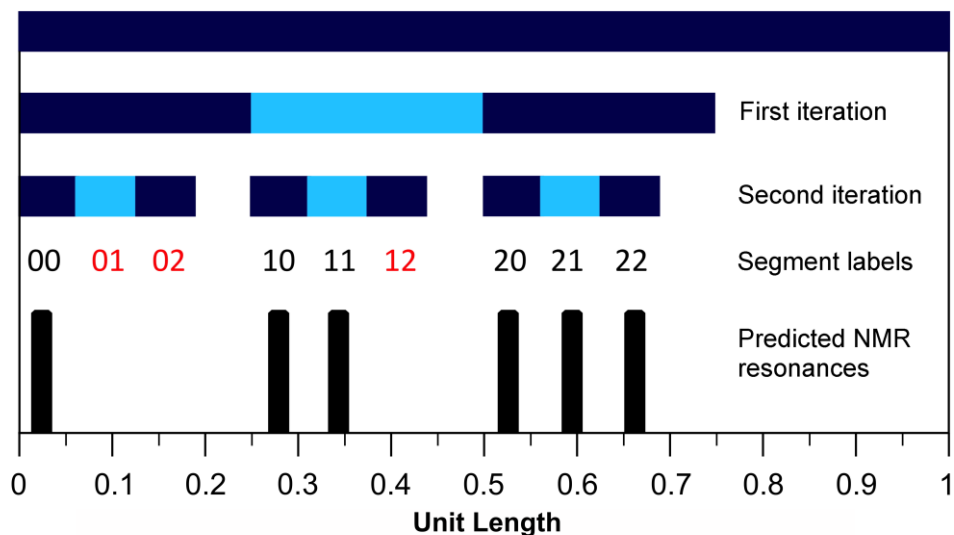


**Figure 6.** Graphical construction of the fourth-quarter Cantor set (first two iterations). This shows how the relative positions of the  $^1\text{H}$  NMR resonances corresponding to the quintet sequences shown in Table 2 emerge from the two-digit codes assigned to each sequence on the basis of a chain-folded "pairwise" binding model for pyrene. This assignment does not generate the codes 01, 02 and 12 (Table 2), so it is predicted that no corresponding NMR resonances will be found at these positions.

Indeed, titration of copolymer **22** against pyrene- $d_{10}$  (Figure 7) resulted in the emergence, above a pyrene:NDI-residue mole ratio of ca. 1:1, of a resonance-pattern [spectrum 7(b), mole ratio 1.6:1] whose relative chemical shifts in the NDI region correspond very closely to those predicted in Figure 6. This result provides strong support for our proposal (Figure 4) that the observed peak in binding strength for the diacid linker with  $x = 2$  is associated with tight chain-folding and "pairwise" binding of each pyrene to two adjacent NDI residues.

Prediction of a complete NMR spectrum requires not only chemical shift values but also resonance intensities. For signals arising from different copolymer sequences, such intensities are directly proportional to sequence-probabilities, but in a 100% random, 1:1 copolymer all

sequences of a given length have the *same* probability. Different resonance intensities would then simply reflect the number of different sequences contributing to each resonance.

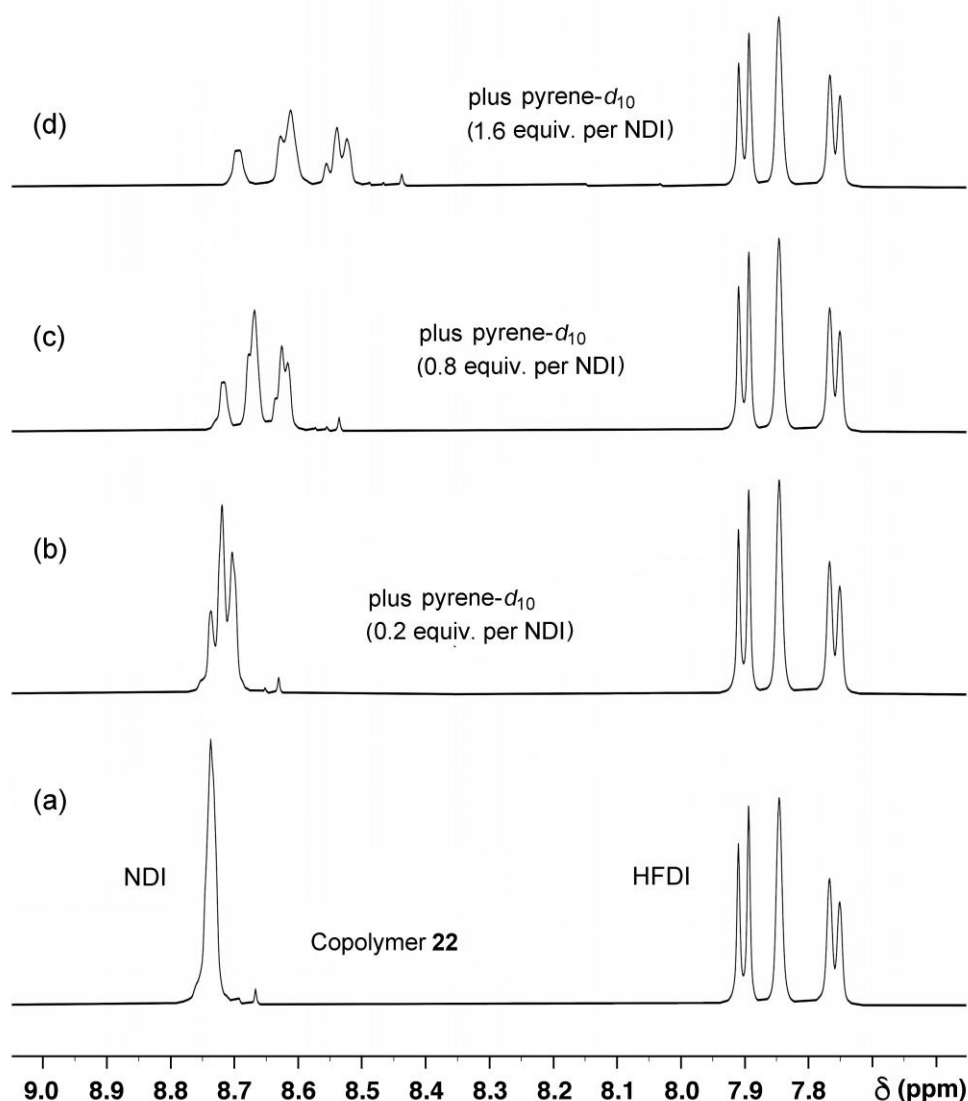


**Figure 7.**  $^1\text{H}$  NMR titration of copolymer **22** in  $\text{CDCl}_3$ /trifluoroethanol (6:1 v/v) against pyrene- $d_{10}$ . As the concentration of pyrene increases, the single NDI ("I") resonance in the absence of pyrene splits into three signals corresponding to the three distinguishable triplet sequences IFI, [IIF+FFI], III. Ultimately, six NDI resonances are seen corresponding to the six groups of quintets shown in Table 2. The very weak resonance at ca. 8.67 ppm in the spectrum of the uncomplexed polymer is assigned to a trace of an NDI-based macrocycle, as it shows a strong upfield shift in the presence of pyrene but no sequence-related splitting. The final concentration of NDI, in spectrum 7(d), was 3.16 mM.

For copolymer **22**, the observed resonance pattern [spectrum 7(d)] can be shown to correspond to a copolymer sequence-distribution having a degree of randomness of ca. 80%.

In a fully random I/F copolymer (1:1 mole ratio) the probability of finding "F" or "I" at any (non-centred) position in an NDI-centred sequence is 0.5, but at 80% randomness the probability of finding "F" at any position in an NDI-centred sequence would be only 0.4, and that of finding "I" 0.6. Since copolymer **22** has overall 1:1 stoichiometry (confirmed by integration of the NMR spectrum), this also implies that the HFDI-centred sequences must contain "F" with probability 0.6 and "I" with probability 0.4. In other words, the copolymer exhibits a degree of blockiness.

On this basis it proved possible to simulate a  $^1\text{H}$  NMR spectrum for the NDI resonances of copolymer **22** in the presence of pyrene, using complexation shifts (Table 2) predicted by Equation 1 and quintet sequence-probabilities calculated on the basis of an 80% degree of randomness (relative to a 1:1 diblock  $[(\text{NDI})_n-(\text{HFDI})_n]$  copolymer having randomness of zero). The simulated spectrum is shown in Figure 8, superimposed on the experimental spectrum [an expanded version of spectrum (9d)]. The agreement is not quite perfect (a very weak splitting of the lowest-field resonance is, for example, unaccounted for) but it is certainly good enough to confirm the hypothesis that the peak in binding energy for pyrene at  $x = 2$  results from tight chain-folding and pairwise binding at adjacent NDI residues. The very weak NDI resonance at highest field (ca. 8.44 ppm in Figure 8) marked "M" is assigned to trace levels of an NDI-based macrocycle, as this resonance also shifts markedly to high field in the presence of pyrene but shows no sequence-related splitting.

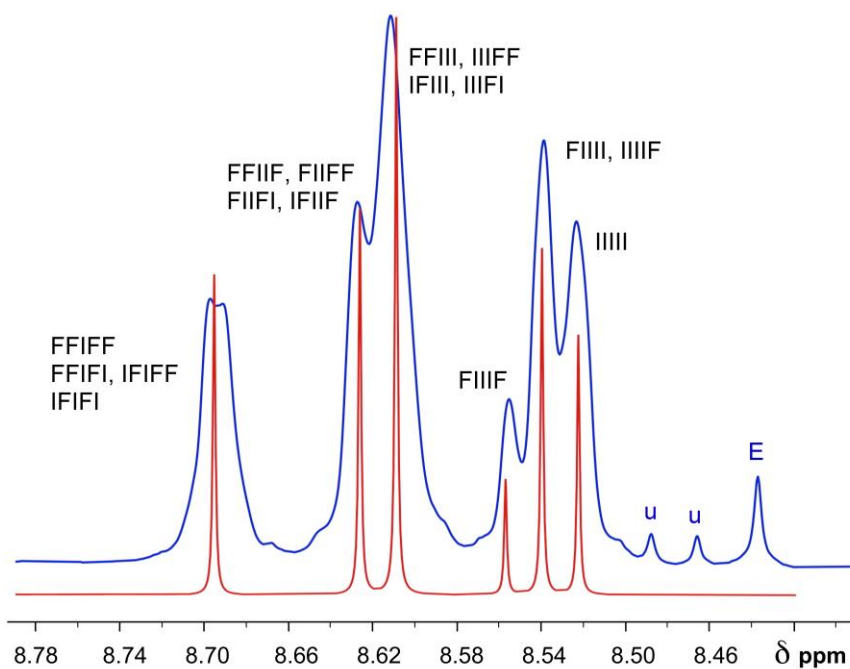


**Figure 8.** Comparison of simulated (red) and experimental (blue)  $^1\text{H}$  NMR resonance patterns (NDI protons only) for copolymer **22** in the presence of 1.6 mole equivalents of pyrene per NDI residue. The simulated spectrum was generated using the total shielding parameters  $T$  (Table 2) for all possible NDI/HFDI quintet sequences, scaled empirically by a value for  $a$  (Equation 1) of 0.368 to afford complexation shifts in ppm. Relative intensities were simulated as sequence-probabilities, calculated on the basis of a copolymer chain in which the sequence-distribution is 80% random relative to a non-random diblock NDI/HFDI copolymer. (E = macrocycle; u = unidentified).

#### 4. Conclusions

Poly(ester-imide)s obtained by polycondensation of *N,N'*-bis(2-hydroxyethyl)naphthalene-1,4,5,8-tetracarboxylic-diimide with the aliphatic diacyl chlorides  $\text{ClOC}(\text{CH}_2)_x\text{COCl}$  ( $x = 1$  to 6) show significant upfield complexation shifts of the diimide resonance in the presence of pyrene and perylene, as a result of supramolecular binding of the polycyclic aromatic molecules at the diimide residues. Pronounced maxima in the complexation shifts with these hydrocarbons are seen for the poly(ester-imide) with  $x = 2$ , due to the presence of a chain fold that is geometrically optimum for a pyrene molecule to intercalate into, making near-van-der-Waals contact with two adjacent diimide residues. "Pairwise" binding of this type was

confirmed by  $^1\text{H}$  NMR studies of pyrene complexation with a copoly(ester-imide), again with  $x = 2$ , but now containing both NDI and HFDI units. The resulting NMR resonance-pattern showing clear evidence of fractal-type character.

## Conflicts of interest

There no conflicts of interest to declare.

## Acknowledgements

This work was supported by the H2020 program of the European Union under the ITN project *Euro-Sequences*, H2020-MSCA-ITN-2014, grant number 642083 (Marie Skłodowska-Curie PhD studentship to MK) and by the Leverhulme Foundation in the UK, grant number EM-2018-0161/4 (Emeritus Fellowship to HMC).

## References

1. F. H. C. Crick, On protein synthesis. *Symp. Soc. Exp. Biol.*, 1958, **12**, 138–163.
2. M. Nirenberg, Historical review: Deciphering the genetic code – a personal account. *Trends Biochem. Sci.*, 2004, **29**, 46–54.
3. C. R. Dawkins, *The Blind Watchmaker*, Longmans, London, 1986, p. 115.
4. H. M. Colquhoun and J.-F. Lutz, Information-containing macromolecules. *Nat. Chem.*, 2014, **6**, 455–456.
5. M. G. T. A. Rutten, F. W. Vaandrager, J. A. A. W. Elemans and R. J. M. Nolte, Encoding information into polymers. *Nat. Rev. Chem.*, 2018, **2**, 367–381.
6. J.-F. Lutz, M. Ouchi, D. R. Liu and M. Sawamoto, Sequence-Controlled Polymers. *Science*, 2013, **341**, 1238149.



7. J.-F. Lutz, J.-M. Lehn, E. W. Meijer and K. Matyjaszewski, From precision polymers to complex materials and systems. *Nat. Rev. Chem.*, 2016, **1**, 1–14.
8. J.-F. Lutz, Defining the field of sequence-controlled polymers. *Macromol. Rapid Commun.* 2017, **38**, 1700582.
9. H. M. Colquhoun and Z. Zhu, Recognition of polyimide sequence-information by a molecular tweezer. *Angew. Chem., Int. Ed.*, 2004, **43**, 5040–5045.
10. H. M. Colquhoun, Z. Zhu, C. J. Cardin, and Y. Gan, Principles of sequence-recognition in aromatic polyimides. *Chem. Commun.*, 2004, 2650–2652.
11. H. M. Colquhoun, Z. Zhu, C. J. Cardin, Y. Gan and M. G. B. Drew, Sterically controlled recognition of macromolecular sequence information by molecular tweezers. *J. Am. Chem. Soc.*, 2007, **129**, 16163–16174.
12. H. M. Colquhoun, Z. Zhu, C. J. Cardin, M. G. B. Drew and Y. Gan, Recognition of sequence-information in synthetic copolymer chains by a conformationally constrained tweezer molecule. *Faraday Discuss.*, 2009, **143**, 205–220.
13. Z. Zhu, C. J. Cardin, Y. Gan, C. A. Murray, A. J. P. White, D. J. Williams and H. M. Colquhoun, Conformational modulation of sequence recognition in synthetic macromolecules. *J. Am. Chem. Soc.*, 2011, **133**, 19442–19447.
14. Z. Zhu, C. J. Cardin, Y. Gan and H. M. Colquhoun, Sequence-selective assembly of tweezer-molecules on linear templates enables frameshift reading of sequence information. *Nat. Chem.*, 2010, **2**, 653–660.
15. J. S. Shaw, R. Vaiyapuri, M. P. Parker, C. A. Murray, K. J. C. Lim, C. Pan, M. Knappert, C. J. Cardin, B. W. Greenland, R. Grau-Crespo and H. M. Colquhoun, Elements of fractal geometry in the <sup>1</sup>H NMR spectrum of a copolymer intercalation-complex: identification of the underlying Cantor set. *Chem. Sci.*, 2018, **9**, 4052–4061.
16. K-W. Lienert, Poly(ester-imide)s for industrial use. *Adv. Polym. Sci.*, 1999, **141**, 45–82.
17. A. A. Shaikh, G. Schwarz and H. R. Kricheldorf, Macrocycles 23. Odd–even effect in the cyclization of poly(ester imide)s derived from catechols. *Polymer*, 2003, **44**, 2221–2230.

18. T. Vlad-Bubulac, C. Hamciuc, and O. Petreus, Synthesis and characterization of some polyesters and poly(ester-imide)s based on bisphenol-A derivatives. *High Perform. Polym.*, 2010, **22**, 345–358.
19. S. J. Meehan, S. W. Sankey, S. M. Jones, W. A. MacDonald and H. M. Colquhoun, Cocrystalline copolyimides of poly(ethylene 2,6-naphthalate). *ACS Macro Lett.*, 2014, **3**, 968–971.
20. M. Hasegawa, S. Takahashi, S. Tsukuda, H. Soichi, T. Hirai, J. Ishii, Y. Yamashina, and Y. Kawamura, Symmetric and asymmetric spiro-type colorless poly(ester imide)s with low coefficients of thermal expansion, high glass transition temperatures, and excellent solution-processability. *Polymer*, 2019, **169**, 167–184.
21. M. Bruma, I. Sava, I. Negulescu, W. Daly, J. Fitch and P. Cassidy, Synthesis and properties of fluorinated poly(ester-imide)s. *High Perform. Polym.*, 1995, **7**, 411–420.
22. N. Zindy, J. T. Blaskovits, C. Beaumont, J. Michaud-Valcourt, H. Saneifar, P. A. Johnson, D. Bélanger, and M. Leclerc, Pyromellitic diimide-based copolymers and their application as stable cathode active materials in lithium and sodium-ion batteries. *Chem. Mater.* 2018, **30**, 6821–6830.
23. C. Kulkarni and S. J. George, Carbonate linkage bearing naphthalenediimides: Self assembly and photophysical properties. *Chem. Eur. J.* 2014, **20**, 4537–4541.
24. B. Aradi, B. Hourahine and T. Frauenheim, DFTB+, a sparse matrix-based implementation of the DFTB method. *J. Phys. Chem. A*, 2007, **111**, 5678–5684.
25. M. Elstner, D. Porezag, G. Jungnickel, J. Elsner, M. Haugk, T. Frauenheim and G. Seifert, Self-consistent-charge density-functional tight-binding method for simulations of complex materials properties. *Phys. Rev. B*, 1998, **58**, 7260–7268.
26. L. Zhechkov, T. Heine, S. Patchkovskii, G. Seifert, and H. A. Duarte, An efficient *a posteriori* treatment for dispersion interaction in density-functional-based tight binding. *J. Chem. Theory Comput.*, 2005, **1**, 841–847.
27. H. J. S. Smith, *Proc. London Math. Soc.*, 1875, **6**, 140–153.